



Novel versatile imine—enamine chemosensor based on 6-nitro-4-oxo-4*H*-chromene for ion detection in solution, solid and gas-phase: synthesis, emission, computational and MALDI-TOF-MS studies

Javier Fernández-Lodeiro^a, Cristina Nuñez^{b,*}, Ricardo Carreira^b, Hugo M. Santos^b, Carlos Silva López^c, Juan Carlos Mejuto^a, José Luís Capelo^{a,b}, Carlos Lodeiro^{a,b,*}

^aPhysical-Chemistry Department, Faculty of Science, Ourense Campus, University of Vigo, 32004, Ourense, Spain

^bREQUIMTE, Department of Chemistry, FCT-UNL, 2829-516 Monte de Caparica, Portugal

^cOrganic-Chemistry Department, Faculty of Chemistry, As Lagoas Marcosende, University of Vigo, 36310, Spain

ARTICLE INFO

Article history:

Received 8 October 2010

Received in revised form 8 November 2010

Accepted 8 November 2010

Available online 18 November 2010

Keywords:

Imines

Enamines

Fluorescent

MALDI-TOF-MS

Metal ions

Chromenes

PPMA supported compound

ABSTRACT

A new versatile emissive molecular probe (**3**) derived from 1,5-bis(2-aminophenoxy)-3-oxopentane bearing two units of 6-nitro-4-oxo-4*H*-chromene- has been prepared by a Schiff-base condensation method using conventional and green, ultrasound-aided, methods. The dry yellow powder was characterized as the imine species (**3**). These imine species, however, were found to rapidly convert to their enamine form (**4**) in solution, under the presence of water traces. This reaction was computationally studied through Density Functional Theory (DFT) in order to investigate the relative stability of the molecular pair **3/4**. The sensing properties of the enamine (**4**) towards various metal ions were investigated via absorption and fluorometric titrations in solution in dichloromethane, acetonitrile and DMSO. The compound shows a fluorescent turn-off response in the presence of Cu²⁺, Zn²⁺, Cd²⁺, Hg²⁺ and Ag⁺ over the other metal ions studied, such as Li⁺, Na⁺, K⁺, Ca²⁺, Co²⁺ and Ni²⁺, being stronger for Cu²⁺ and Hg²⁺. The gas phase chemosensing abilities of (**3**) were also explored suggesting (**3**) as new active MALDI-TOF-MS matrix by two dry methods showing a strong selectivity towards Cu²⁺ and Ag⁺. Our preliminary results show promising uses of (**3**) supported in PPMA films as metal ion solid chemosensor.

© 2010 Elsevier Ltd. All rights reserved.

1. Introduction

Chemosensors are natural or artificial systems including a receptor fragment, which is capable of selectively interacting with a substrate, a signalling fragment and some times a linker connecting them.¹ Among all the chemosensors, fluorescent probes are particularly important due to their intrinsic sensitivity.²

The chiral chromene unit is the core structure of a number of natural products³ and is used as a versatile synthon in heterocyclic chemistry as well as in pharmaceutical industry. These systems exhibit a wide range of biological properties,^{4–9} for example, diuretic, anticoagulant and anti-anaphylactic activity.^{10,11} They also have interesting photochemical properties,¹² and are used as colorimetric probes.¹³

The synthetic significance of 3-formylchromone derivatives raises from their usefulness as reactive agents and valuable precursors

for many different heterocycles. They contain three electron deficient sites (C-2, C-4 and CHO) suitable for nucleophilic attack and, as a consequence of competition between these centers, various types of compounds can be formed upon the reaction of 3-formylchromones with strong nucleophiles.¹⁴ In general, 3-formylchromones readily react with primary amines in an alcoholic medium yielding an enamine-adduct, which rarely reacts further to give the corresponding Schiff-base.^{12,15a}

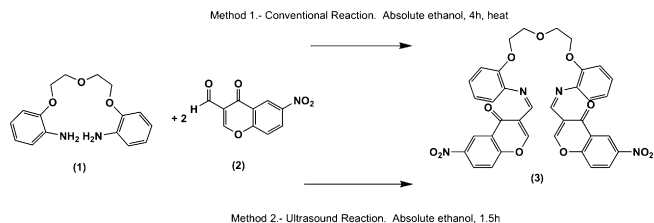
The present investigation aims to develop a multifunctional chemosensor furnished with reactive chromene groups for metal cation detection in solution as well as in gas phase. As a part of our ongoing research in the design and synthesis of new versatile dual chemosensors,¹⁶ fluorescent probes in solution and active-recognition matrices in gas-phase, we report here the synthesis, characterization and studies of a new fluorescence ligand containing two emissive 6-nitro-4-oxo-4*H*-chromene units (**3**) and the corresponding enamine (**4**). The presence of a complex chelating unit formed by four oxygen atoms of the chromene units, two imine nitrogens and the three oxygen atoms of a flexible poly-oxa chain,¹⁷ gives the molecule strong recognition capability towards metal ions

* Corresponding authors. Tel.: +34 988 368894; fax: +34 988 387001 (C.L.); tel.: +351 21 2948300; fax: +351 21 2948550 (C.N.); e-mail addresses: cristina.nunez@dq.fct.unl.pt (C. Nuñez), clodeiro@uvigo.es (C. Lodeiro).

through formation of coordination compounds. Moreover, when the imine compound (**3**) converts to the enamine structure (**4**) the receptor presents two hydroxyl groups, which also allow increasing the coordination capability of the system and introduce new photophysical properties as the excited state internal proton transfer (ESIPT), mechanism. Some solid metal complexes and doped polymeric materials have also been synthesized and characterized in order to explore (**3**) as precursor of new fluorescent hybrid materials.

2. Results and discussion

Probe (**3**) was synthesized following a one-pot reaction, by direct condensation of 1,5-bis(2-aminophenoxy)-3-oxapentane¹⁷ and the commercial carbonyl precursor 6-nitro-4-oxo-4*H*-chromene-3-carbaldehyde. The reaction was performed by a conventional method, heating an ethanolic solution during 4 h and by a green method, using a Branson 1510 E-MT ultrasound bath during 1.5 h. Both methods led to formation of the final product (**3**), which could be isolated as an air-stable yellow solid, with ca. 90–92% yield. The reaction pathway is shown in Scheme 1.



Scheme 1. Synthesis of chemosensor (**3**).

The elemental analysis of the Schiff-base (**3**) isolated as a dry yellow powder confirmed the purity of our sample. The infrared spectrum (in KBr) in both cases shows bands at 1647 and 1640 cm^{-1} , respectively, corresponding to the imine bond $\nu(\text{C}=\text{N})$, and no peaks attributable to unreacted amine or carbonyl groups were present. A band attributable to the C–O–C flexible chain can be also observed at 1257 cm^{-1} in both spectra. The matrix assisted laser desorption time-of-flight mass (MALDI-TOF-MS) spectrum of (**3**) shows a parent peak at 691.52 m/z , corresponding to the protonated imine form of the ligand [**3H**]⁺ obtained irradiating the sample at 337 nm by a N_2 laser, (see Fig. 1) with no evidence of peaks at 726.18 m/z corresponding to the enamine form (**4**).

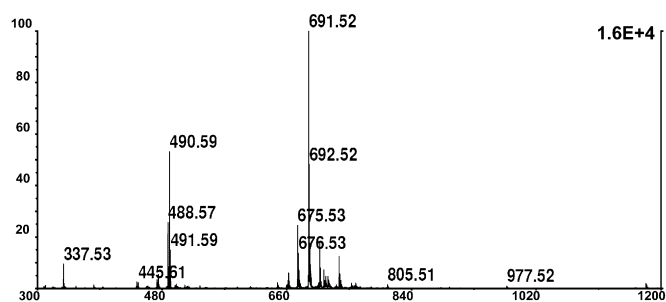
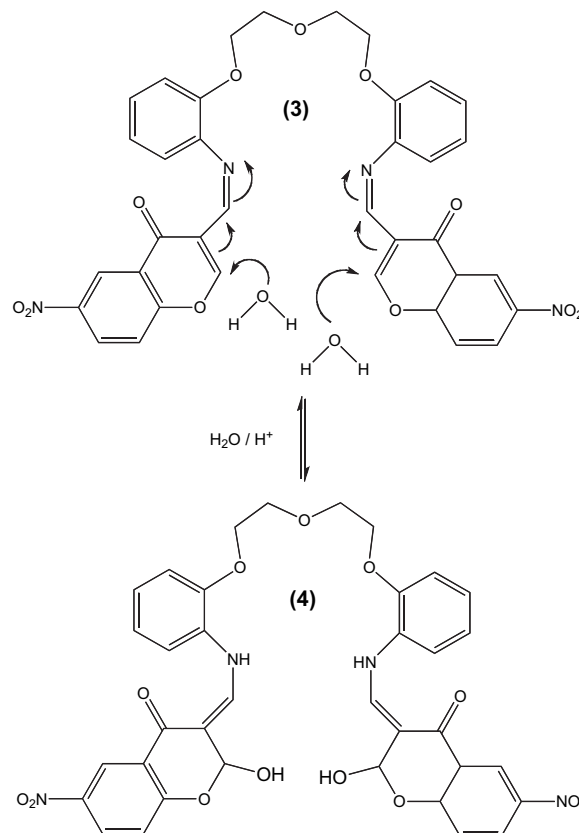


Fig. 1. MALDI-TOF-MS mass spectrum of compound (**3**).

The ^1H and ^{13}C NMR spectra of compound (**3**) were recorded using $\text{DMSO}-d_6$ as solvent. Proton signals were assigned upon standard 2D homonuclear (COSY) and $^1\text{H}/^{13}\text{C}$ heteronuclear (HMQC) spectra. As it could be expected for a Schiff-base, the ^1H NMR spectrum of compound (**3**) in $\text{DMSO}-d_6$ does not show any

peak at ca. 8–9 ppm corresponding to the imine protons. This result confirms that, in solution, the enamine species (**4**) is formed as a more stable compound. It is well known that chromones are efficiently converted in protolytic solvents at room temperature into enamine-type compounds with a typical lemon-yellow colour.¹⁸ The stability of these species in solution was explained by the formation of a hydrogen bonding between the carbonyl oxygen of the pyrone group and the hydrogen atom of the NH group. This behaviour was observed in other similar systems (See Scheme 2).¹⁹



Scheme 2. Conversion of compound (**3**) in (**4**) in the presence of traces of water.

In the ^1H NMR spectrum, the aromatic hydrogen atoms were observed as multiple signals in the aromatic region of the spectrum, while the protons of the ethylene bridges appeared as triplets in the aliphatic region of the spectrum. The signals assigned to the hydroxyl groups appeared at 6.0 ppm as singlet and at 12.0 ppm a singlet signal was observed for the amine proton. Upon addition of D_2O to the sample, the signal assigned to the amine protons disappeared and, in this case, the proton signal of the hydroxyl groups remains because the hydrogen–deuterium exchange is slower.

The imine species (**3**) seems to be unstable upon solvation. Experimental evidence supports that chromone units in (**3**) readily add a water molecule to form an enamine structure yielding (**4**). Density functional calculations also support these conclusions. The calculated free energy of hydration at the M06-2X/631+g(d,p) is -2.88 kcal/mol per chromone unit, which is consistent with a quantitative shift of the hydration/dehydration equilibrium towards the enamine (**4**) form. Furthermore, the existence of more hydrogen bond donors and acceptors in the enamine counterpart should render it even more stable under protic medium (Scheme 2).

The presence of seven potential donor atoms (N_2O_5) in the ligand structure of (**3**), gives strong recognition ability towards metal ions. In order to explore the potential uses in the synthesis of new emissive materials, some solid metal complexes were synthesized

by direct reaction between ligand (**3**) and $\text{Cu}(\text{BF}_4)_2 \cdot 6\text{H}_2\text{O}$, $\text{Zn}(\text{ClO}_4)_2 \cdot 6\text{H}_2\text{O}$, $\text{Ag}(\text{CF}_3\text{SO}_3)_2 \cdot \text{H}_2\text{O}$, $\text{Cd}(\text{ClO}_4)_2 \cdot \text{H}_2\text{O}$ and $\text{Hg}(\text{CF}_3\text{SO}_3)_2 \cdot \text{H}_2\text{O}$ metal salts. Addition of the metal salt dissolved in acetonitrile to a stirred solution of (**3**) in the same solvent gave in all cases analytically pure mononuclear complexes. The photophysical characterization of all complexes is summarized in Table 1.

Table 1

Optical data for (**3**), (**4**) and the metal complexes of compound (**3**) in acetonitrile ($\lambda_{\text{exc}}=399 \text{ nm}$; 298 K)

Metal complex	λ_{max} (nm); log ϵ	λ_{em} (nm)	$\Delta\lambda$ (nm)	ϕ	λ_{em} (nm) solid state
(3)	—	—	—	—	545
[Cu 3](BF_4) $_2 \cdot 5\text{H}_2\text{O}$	388; 4.41	471	83	<0.001	—
[Zn 3](ClO_4) $_2 \cdot 1\text{H}_2\text{O}$	393; 4.46	484	91	<0.001	—
[Cd 3](ClO_4) $_2 \cdot 6\text{H}_2\text{O}$	387; 4.47	497	110	<0.001	535
[Ag 3](CF_3SO_3) $_2 \cdot 3\text{H}_2\text{O}^a$	386; 4.20	463	77	<0.001	542
[Hg 3](CF_3SO_3) $_2 \cdot 3\text{H}_2\text{O}^a$	384; 4.32	464	80	<0.001	—

^a DMSO solution.

It is important to mention that despite compound (**3**) being maintained in solution during 4 h, the IR spectra and the MALDI-TOF-MS spectra of each complex shows clearly the signals attributed to the imine bond vibration and the (**3**) M peaks, respectively. This result evidences the reversible equilibrium between the imine (**3**) and enamine (**4**) species after drying the complexes under vacuum.

In order to explore the application of chemosensor (**3**) as molecular probe for metal ions in gas phase, several MALDI-TOF-MS titrations were performed. Compound (**3**) dissolved in acetonitrile without any additional MALDI matrix was titrated with six different transition and post-transition metal ions, such as Co^{2+} , Ni^{2+} , Cu^{2+} , Zn^{2+} , Hg^{2+} and Ag^+ in molar ratios ligand/metal 1:1 and 1:2.

To perform the metal titrations, two different strategies were explored: a dried droplet solution and a layer-by-layer deposition sample preparation. First, two solutions containing compound (**3**) (1 μL) and the metal salt (1 μL) were mixed and shaken and then applied in the MALDI-TOF-MS sample holder. The second method consisted of a layer by layer addition of different solutions: (i) a solution of (**3**) was spotted in the MALDI-TOF-MS plate and then dried in vacuum; subsequently, 1 μL of the solution containing the metal salt was placed on the sample holder and dried. Finally, the plate was then inserted in the ion source. For this second case, the complexation reaction between the ligand and the metal salts occurred in the holder, and the complex species were produced in gas phase.

The ligand peak in the MALDI-TOF-MS appears always at 691.52 m/z ; this peak can be unambiguously attributed to the protonated species [**3**H] $^+$. No peak corresponding to (**4**) with 726.6 m/z was detected. By both methods of sample preparation, upon addition of 1 equiv of Ag^+ , the peak attributable to the ligand disappears, and a new peak with 100% of intensity appears at 799.49 m/z (by layer-by-layer deposition) and with 100% of intensity appears at 798.35 m/z (by solution sample). This peak corresponds to the mononuclear species [**3**Ag] $^+$ (see Fig. 2). Once again upon drying under vacuum the sample holder the enamine (**4**) was always transformed into the imine (**3**) as can be observed in the spectra.

In the copper(II) titration, the peak assignable to the mononuclear [**3**Cu] $^+$ species was observed upon addition of 1 equiv of Cu^{2+} with 100% of intensity at 753.60 m/z (by layer-by-layer deposition) and 753.57 m/z (by solution sample). A second peak at 834.66 m/z (by layer-by-layer deposition) and 834.63 m/z (by solution sample), attributable to the dinuclear species [**3**Cu $_2$ (H $_2$ O)] $^+$ also was detected (see Fig. 3).

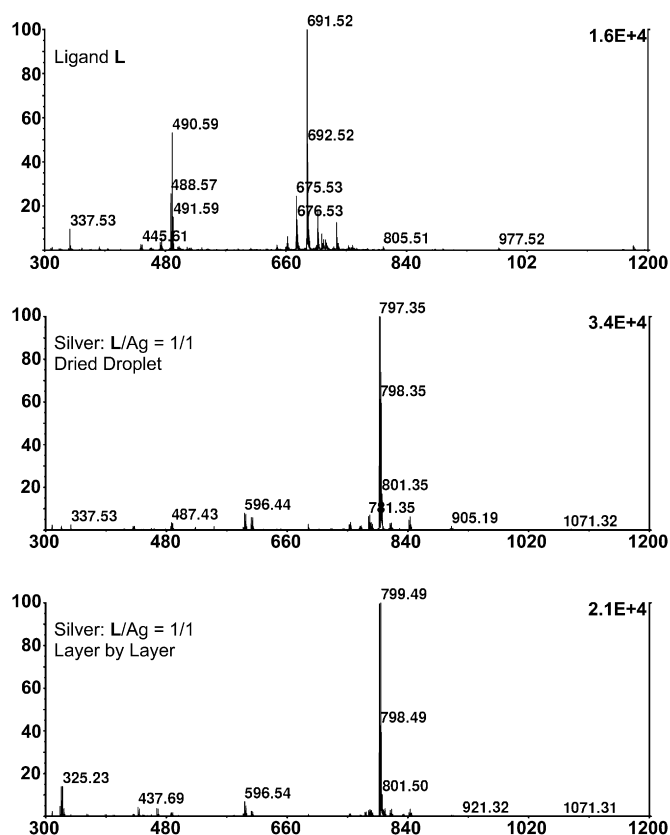


Fig. 2. MALDI-TOF-MS mass spectra of compound (**3**) after titration with $\text{Ag}(\text{CF}_3\text{SO}_3)_2 \cdot \text{H}_2\text{O}$ (1 equiv of metal) using two methods: a dry droplet and layer-by-layer deposition.

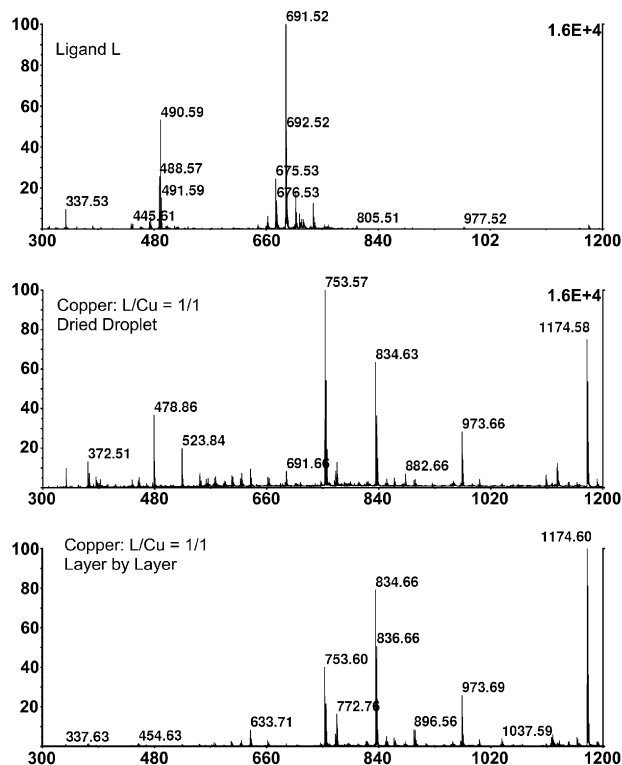


Fig. 3. MALDI-TOF mass spectra of compound (**3**) after titration with $\text{Cu}(\text{BF}_4)_2 \cdot 6\text{H}_2\text{O}$, (1 equiv of metal) using two methods: a dry droplet and a layer-by-layer deposition.

In both metal titrations and by both analytical methods explored it is important to mention that the peak assignable to the protonated ligand at 691.5 m/z disappears.

In the other metal titrations, peaks with low intensity at 795.60 and 767.54 m/z corresponding to $[3\text{CoEtOH}]^+$ and $[3\text{NiH}_2\text{O}]^+$, respectively, were observed when compound (**3**) was titrated in the same conditions with a stoichiometric quantity of Co^{2+} or Ni^{2+} suggesting less stability of the complexes formed in the technique. In all cases the peak attributed to the protonated ligand $[3\text{H}]^+$ was observed as the most intense. In the case of Zn^{2+} and Hg^{2+} titrations any peak corresponding to the metal complex was detected. The results suggest that (**3**) can be used to sense these metal ions by MALDI-TOF-MS with high selectivity towards Cu^{2+} and Ag^+ .

The absorption, emission and excitation spectra of (**4**) were studied in aprotic solvents, such as CHCl_3 , DMSO and CH_3CN at 298 K. The results in CHCl_3 are reported in Fig. 4.

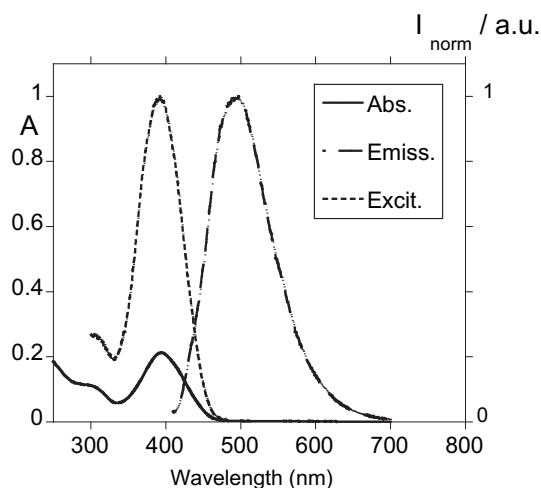


Fig. 4. Absorption, emission and excitation spectra of compound (**4**) in CHCl_3 solution at room temperature. ($\lambda_{\text{exc}}=390$ nm; $\lambda_{\text{em}}=510$ nm, $[\text{L}]=1.00 \cdot 10^{-6}$ M).

The absorption spectrum shows two bands with the maxima centered at 291 and 398 nm, coincident with the excitation spectrum. These bands appear in the same spectral region as other chromenes reported in the literature. The fluorescence emission spectrum of (**4**) presents a band centered at 500 nm, with weak intensity assigned to the chromene emission.²⁰ The relative fluorescence quantum yield obtained in DMSO solution using a quinine solution as reference was in the range of 10^{-3} M. This low emission could be due to the presence of the nitro group in the chromene units,²⁰ and to the photophysical internal ESIP and PET deactivation mechanisms.²¹

The lower intensity emission observed in the coordinative solvents DMSO and CH_3CN prevent further complexation studies in these solvents and due to this all complexation studies were developed only in CHCl_3 .

In order to explore the chemosensor ability of the enamine species (**4**) in solution, the effect of metal cations, such as Cu^{2+} , Zn^{2+} , Cd^{2+} , Hg^{2+} and Ag^+ on the absorption, and the fluorescence spectra was studied in CHCl_3 as solvent.

Fig. 5 depicts the absorption and emission spectra of a solution of (**4**) in the presence of increasing amounts of $\text{Cu}(\text{BF}_4)_2$ dissolved in acetonitrile. Upon addition of 14 equiv of metal ion, the absorption band centered at 398 nm shows an intense absorption decrease effect, and the fluorescence emission observed at 500 nm was totally quenched.

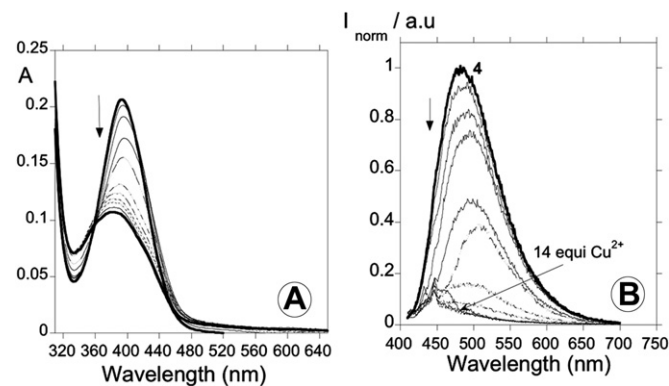


Fig. 5. Absorption (left) and emission (right) titration of chloroform solutions of (**4**) as a function of increasing amounts of $\text{Cu}(\text{BF}_4)_2 \cdot 6\text{H}_2\text{O}$. ($[\text{4}]=1.00 \cdot 10^{-5}$ M for absorption and $[\text{4}]=7.923 \cdot 10^{-6}$ M for emission, $\lambda_{\text{exc}}=389$ nm).

After the addition of $\text{Hg}(\text{CF}_3\text{SO}_3)_2 \cdot \text{H}_2\text{O}$, $\text{Zn}(\text{ClO}_4)_2 \cdot 6\text{H}_2\text{O}$, $\text{Cd}(\text{ClO}_4)_2 \cdot \text{H}_2\text{O}$ and $\text{Ag}(\text{CF}_3\text{SO}_3) \cdot \text{H}_2\text{O}$ to (**4**), a similar quenching on the fluorescence emission was observed; but contrary to copper(II), which only required a few equivalents of metal to turn-OFF the emission, in these cases 23, 83, 1200 and 1400 equiv were necessary, respectively (see Fig. 6).

On the other hand, no changes were observed in the absorption and emission spectra of ligand (**4**) with the addition of Li^+ , Na^+ , K^+ and Ca^{2+} in our conditions.

This turn-OFF effect observed on the luminescence upon metal complexation with Cu^{2+} and Hg^{2+} is consistent with a chelation enhancing of the quenching effect (CHEQ), when coordination induces a photoinduced energy transfer that quench the π^* emissive state through low-lying metal-centered states.²²

More interestingly, metals, such as Zn^{2+} , Cd^{2+} or Ag^+ with fully filled electron shells usually enhance the fluorescence upon chelation, by CHEF effect, however in our case the quenching observed can be ascribed to the strong excited state internal proton transfer (ESIP) from the two OH groups present in the enamine species (**4**) to the excited chromophores. Previous studies reported by us with an emissive ligand bearing two β -naphthol units shows similar emission intensity in compare with (**3**).²³

The stability constants for the interaction of (**4**) with Cu^{2+} , Hg^{2+} and Zn^{2+} were calculated using HypSpec software and are summarized in Table 2.²⁴ Unfortunately, for Cd^{2+} and Ag^+ it was not possible to calculate the stability constants using HypSpec.

Taking into account the values reported in Table 2, the sequence of the strongest interaction expected for sensor (**4**), in decreasing order is $\text{Hg}^{2+} > \text{Zn}^{2+} \approx \text{Cu}^{2+} > \text{Cd}^{2+} = \text{Ag}^+$.

Once the Schiff-base species (**3**) is rapidly converted into the enamine (**4**) in the presence of water-traces in solution, we tried to encapsulate the emissive dye (**3**) into a polymeric matrix in order to compare the fluorescence emission in the solid state as powder and in the polymethylmethacrylate (PPMA) in the absence of water. This strategy is commonly applied for emissive lanthanide complexes that increase the luminescence and brightness in the absence of water.²⁵ This new emissive hybrid inorganic–organic material could be also explored as new metal ion chemosensors.

Taking this strategy in mind, compound (**3**) and all metal complexes were studied in solid state using a optic fibre device connected to the spectrofluorimeter. As it can be seen in Fig. 7A, the emission of the free ligand observed at 545 nm is quenched by the presence of Cu^{2+} , Zn^{2+} and Hg^{2+} as were observed in solution. In the solid state the Cd^{2+} and Ag^+ complexes are highly emissive showing the typical CHEF effect in compare with the free (**3**) in powder. The fluorescence band for the ligand appears

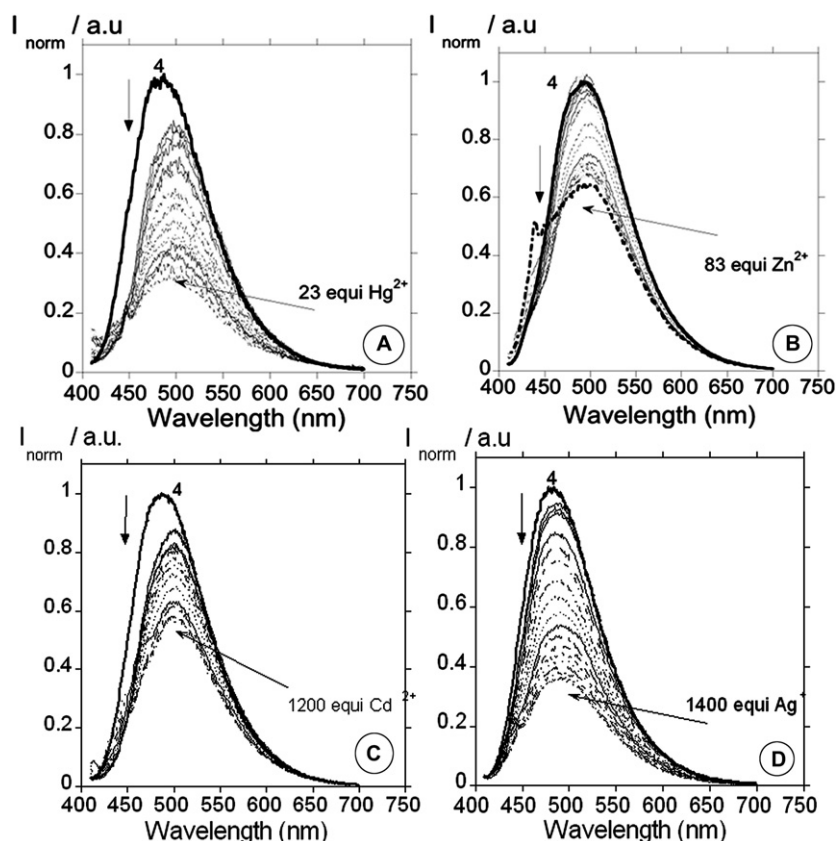


Fig. 6. Emission titration spectra of a chloroform solution of (**4**) as a function of increasing amounts of Hg^{2+} , Zn^{2+} , Cd^{2+} and Ag^+ . ($[\mathbf{4}] = 1.00 \cdot 10^{-5}$ M, $\lambda_{\text{exc}} = 389$ nm).

Table 2

Stability constants for compound (**4**) in the presence of Cu^{2+} , Zn^{2+} and Hg^{2+} ions in CH_3CN or CHCl_3 . (M:L)

Ligand	Interaction	$\log K(\text{Absorption})$	$\log K(\text{Emission})$
4 ^a	Cu^{2+} (1:1)	$2.46 \pm 4.3 \times 10^{-2}$	$2.41 \pm 4.3 \times 10^{-2}$
4 ^a	Hg^{2+} (1:1)	$4.66 \pm 2.4 \times 10^{-3}$	$4.21 \pm 6.5 \times 10^{-3}$
4 ^b	Cu^{2+} (1:1)	$1.24 \pm 2.6 \times 10^{-3}$	$1.24 \pm 4.3 \times 10^{-2}$
4 ^b	Hg^{2+} (1:1)	$4.68 \pm 2.5 \times 10^{-3}$	$4.10 \pm 2.0 \times 10^{-2}$
	Hg^{2+} (2:1)	$3.34 \pm 2.4 \times 10^{-3}$	$3.25 \pm 2.0 \times 10^{-2}$
4 ^b	Zn^{2+} (1:1)	$2.44 \pm 2.1 \times 10^{-3}$	$2.56 \pm 2.1 \times 10^{-3}$

^a CH_3CN .

^b CHCl_3 .

red-shifted when compare to the solution studies, while the strong emissive PPMA doped films shows a blue-shift band in 40 nm.

Spraying a water solution containing Hg^{2+} , Cd^{2+} or Cu^{2+} (ca. 5×10^{-2} M) over the PPMA solid films (Fig. 8) and dried with air shows clearly an interaction with the ligand, and as consequences the fluorescence emission was quenched in all cases. This preliminary result clearly shows a promising application of compound (**3**) in PPMA support as new solid supported metal chemosensor. Fig. 7B shows the decrease observed in the PPMA doped film after 15, 30 and 60 min of exposure to Cu^{2+} .

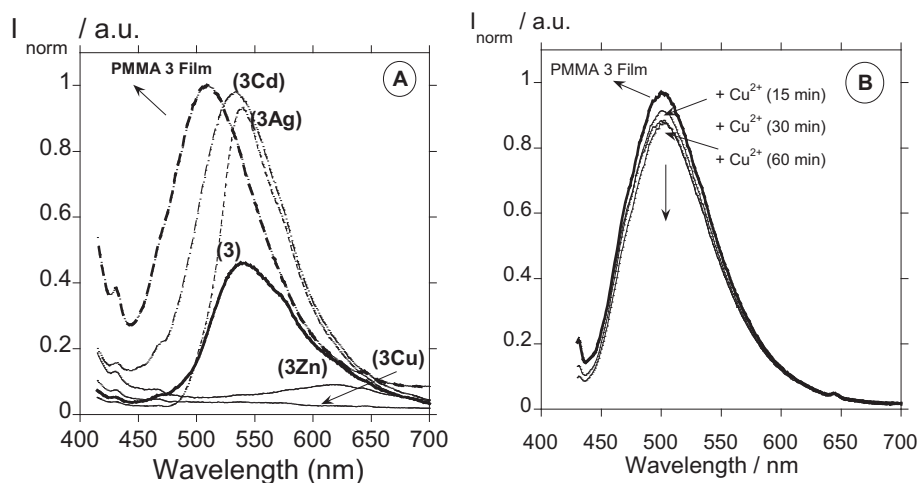


Fig. 7. (A) Emission spectra in solid state of (**3**), PPMA doped film with **3** and the Cu^{2+} , Zn^{2+} , Cd^{2+} and Ag^+ solid metal complexes. (B) Emission spectra of the PPMA doped film with compound **3** and after spraying Cu^{2+} (Dried films after 15, 30 and 60 min, $\lambda_{\text{exc}} = 390$ nm).

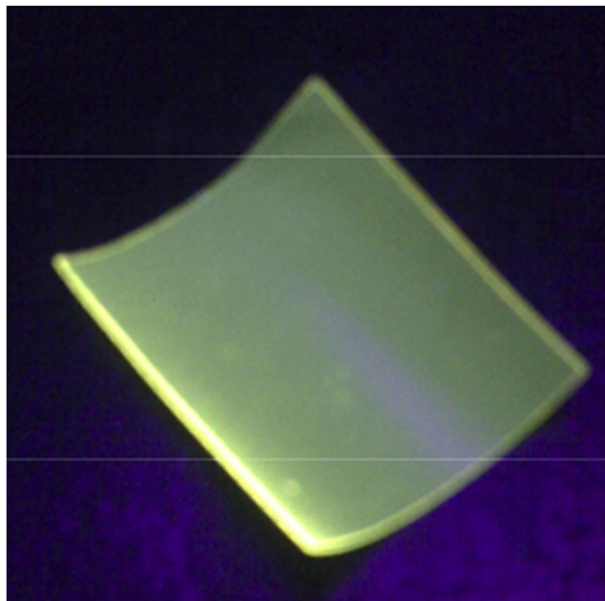


Fig. 8. PPMA doped film with (3) under UV irradiation. ($\lambda_{\text{exc}}=366$ nm).

3. Conclusions

By a simple and green synthetic method a new multifunctional ligand containing two nitro-cromene units (3) were successfully synthesized and characterized. Experimental and computational evidence show that two chemical forms of the ligand occur depending of the physical state: the imine form (3) in solid state and gas phase, and the enamine form (4) in solution.

The effect of cations, such as Co^{2+} , Ni^{2+} , Cu^{2+} , Cd^{2+} , Zn^{2+} , Ag^{+} and Hg^{2+} , on the absorption, fluorescence and MALDI-TOF-MS spectra was explored. To conduct spectrophotometric analyses, the ligand was dissolved in CHCl_3 , DMSO or acetonitrile and titrated with the analytes. A remarkable selectivity towards Cu^{2+} and Hg^{2+} was observed in the solution studies and towards Ag^{+} and Cu^{2+} by the MALDI-TOF-MS analyses.

Some Metal complexes with Cu^{2+} , Zn^{2+} , Cd^{2+} , Ag^{+} and Hg^{2+} were synthesized and characterized in order to compare with the results obtained in solution by absorption and fluorescence spectroscopy.

Finally PPMA doped films were prepared with compound (3) in order to explore the potential application of (3) as solid supported fluorescence chemosensor for metal ions. Our preliminary results show promising uses of (3) supported in PPMA films as metal ion solid chemosensor.

4. Experimental section

4.1. Materials and general methods

Elemental analyses were carried out at the REQUIMTE DQ Service (Universidade Nova de Lisboa), on a Thermo Finnigan-CE Flash-EA 1112-CHNS instrument and in the CACTI, University of Vigo Elemental analyses Service on a Fisons EA-1108 analyser. Infrared spectra were recorded as KBr discs using Bio-Rad FTS 175-C spectrophotometer. Proton NMR spectra were recorded using a Bruker WM-400 MHz spectrometer.

MALDI-TOF-MS analysis were performed in a MALDI-TOF-MS model voyager DE-PRO biospectrometry workstation equipped with a nitrogen laser radiating at 337 nm from Applied Biosystems

(Foster City, United States) at the REQUIMTE DQ, Universidade Nova de Lisboa. The acceleration voltage was 2.0×10^4 kV with a delayed extraction (DE) time of 200 ns. The spectra represent accumulations of 5×100 laser shots. The reflectron mode was used. The ion source and flight tube pressures were less than 1.80×10^{-7} and 5.60×10^{-8} Torr, respectively. The MALDI mass spectra of the soluble samples (1 or 2 $\mu\text{g}/\mu\text{L}$), such as the ligand and metal complexes were recorded using the conventional sample preparation method for MALDI-MS.

The MALDI mass spectra of the soluble samples (1 or 2 $\mu\text{g}/\mu\text{L}$), such as metal salts were recorded using two sample preparation methods for MALDI-MS: 'dried droplet' and 'layer by layer'.

The 'dried droplet' standard MALDI sample preparation is very simple. Here, the sample and matrix are dissolved in a common solvent or solvent system, and mixed either before deposition onto or directly on the MALDI sample support. The matrix-analyte droplet of typically 1 μL is then slowly dried in air, or under a forced flow of cold air. This results in a deposit of crystals, which depending on the matrix; vary between sub micrometer and several hundred micrometers in size. The 'layer by layer' method involves the use of fast solvent evaporation to form the first layer of small matrix crystals, followed by deposition of the analyte solution (metals) on top of the crystal layer.²⁶

UV/vis absorption spectra (200–800 nm) were performed using a JASCO-650 UV/vis spectrophotometer and fluorescence spectra on a HORIBA JOVIN-IBON Spectramax 4. The linearity of the fluorescence emission versus concentration was checked in the concentration range used (10^{-5} – 10^{-6} M). A correction for the absorbed light was performed when necessary. All spectrofluorimetric titrations were performed as follows: a stock solution of the ligand (ca. 1.00×10^{-3} M) were prepared by dissolving an appropriate amount of the ligand in a 50 mL volumetric flask and diluting to the mark with CHCl_3 , DMSO or CH_3CN UVA–so. The titration solutions ($[\mathbf{4}] = 1.00 \times 10^{-6}$ and 1.00×10^{-5} M) were prepared by appropriate dilution of the stock solution. Titrations were carried out by addition of microliter amounts of standard solutions of the ions dissolved in DMSO or CH_3CN .

Fluorescence spectra of solid samples were recorded using a fibre optic system connected to the Horiba-Jovin Ybon Fluoromax 4 spectrofluorimetric exciting at appropriated λ (nm) the solid compounds. All the measurements were performed at 298 K. Luminescence quantum yields were measured using a solution of quinine sulfate in sulfuric acid (0.5 M) as a standard [ϕ]=0.54 and were corrected for different refraction indexes of solvents.²⁷

4.2. Synthesis of chemosensor (3)

4.2.1. Conventional method. A solution of 1,5-bis(2-amino-phenoxy)-3-oxopentane (0.1974 g, 0.6838 mmol) in ethanol (20 mL) was added dropwise to a refluxing solution of 6-nitro-4-oxo-4H-chromene-3-carbaldehyde (0.315 g, 1.43 mmol) in the same solvent. The resulting solution were gently refluxed with magnetic stirring for ca. 4 h at room temperature and then evaporated to dryness. The residues were extracted with water–chloroform. The organic phase was dried (MgSO_4), filtered and solvent removal gave a yellow powder precipitate, which was then filtered off, washed with cold absolute ethanol and cold diethyl ether and dried under vacuum. After purification by chromatography column, the compound was characterized as (3).

4.2.1.1. Compound (3). Yellow solid (92%). Anal. Calcd for $\text{C}_{36}\text{H}_{30}\text{N}_4\text{O}_{11} \cdot \text{H}_2\text{O}$: C, 60.62; H, 4.53; N, 7.81. Found: C, 60.61; H, 4.83; N, 7.41. MALDI-TOF/MS, $[\text{LH}]^+ = 691.37$. IR (KBr) 3410 $\nu(\text{N-H})_{\text{st}}$, 1647 $\nu(\text{C=N})_{\text{imin}}$, 1257 $\nu(\text{C-O})$, 944 $\nu(\text{C-O-C})$. ^1H NMR (400 MHz) in DMSO of compound 4: δ (ppm) 4.1 (t, 4H₁), 4.4 (t, 4H₂), 7.4 (m,

4H_{4,6}), 7.3 (m, 2H₅), 7.1 (m, 2H₇), 12.0 (s, 2H₉), 6.9 (m, 2H₁₀), 8.3 (m, 2H₁₄), 8.4 (m, 2H₁₆), 8.2 (m, 2H₁₇), 6.8 (m, 2H₁₉), 6.0–6.1 (s, 2H₂₀). ¹³C NMR (100 MHz) in CD₃CN: 69.20 (C₁), 69.30 (C₂), 147.15 (C₃), 114.17 (C₄), 119.25 (C₅), 114.06 (C₆), 113.11 (C₇), 141.78 (C₈), 124.49 (C₁₀), 141.74 (C₁₁), 176.91 (C₁₂), 102.48 (C₁₃), 128.53 (C₁₄), 122.30 (C₁₅), 121.17 (C₁₆), 144.91 (C₁₇), 159.93 (C₁₈), 121.22 (C₁₉).

4.2.2. Green ultrasound synthesis (US). A solution of 1,5-bis(2-aminophenoxy)-3-oxopentane (0.1351 g, 0.46 mmol) and 6-nitro-4-oxo-4H-chromene-3-carbaldehyde (0.2074 g, 0.93 mmol) in ethanol (40 mL) was placed in an ultrasound bath during half an hour at room temperature. The yellow powder precipitate formed was filtered off, washed with cold absolute ethanol and cold diethyl ether and dried under vacuum. After purified the compound by chromatography column, was characterized as compound **(3)**.

4.2.2.1. Compound (3). Yellow solid (82%). Anal. Calcd for C₃₆H₃₀N₄O₁₁·H₂O: C, 60.62; H, 4.53; N, 7.81. Found: C, 60.55; H, 4.05; N, 7.33. MALDI-TOF/MS, [LH]⁺=691.37 (100%). IR (KBr) 3410 ν(N–H)_{st}, 1647 ν(C=N)_{imin}, 1257 ν(C–O), 944 ν(C–O–C). ¹H NMR (400 MHz) in DMSO of compound **4**: δ (ppm) 4.1 (t, 4H₁), 4.4 (t, 4H₂), 7.4 (m, 4H_{4,6}), 7.3 (m, 2H₅), 7.1 (m, 2H₇), 12.0 (s, 2H₉), 6.9 (m, 2H₁₀), 8.3 (m, 2H₁₄), 8.4 (m, 2H₁₆), 8.2 (m, 2H₁₇), 6.8 (m, 2H₁₉), 6.0–6.1 (s, 2H₂₀). ¹³C NMR (100 MHz) in CD₃CN: 69.20 (C₁), 69.30 (C₂), 147.15 (C₃), 114.17 (C₄), 119.25 (C₅), 114.06 (C₆), 113.11 (C₇), 141.78 (C₈), 124.49 (C₁₀), 141.74 (C₁₁), 176.91 (C₁₂), 102.48 (C₁₃), 128.53 (C₁₄), 122.30 (C₁₅), 121.17 (C₁₆), 144.91 (C₁₇), 159.93 (C₁₈), 121.22 (C₁₉).

4.3. Synthesis of metal complexes of **(3)**

A solution of the corresponding metal salt (0.146 mmol) dissolved in acetonitrile (10 mL) was added to a warmed solution of **(3)** (0.146 mmol) in the same solvent (50 mL). The resulting mixture was stirred during 4 h heating gently. A precipitate was formed, which was then filtered off, washed with cold diethyl ether and dried under vacuum line for 3 h. All the compounds are soluble in chloroform, acetone, DMSO, acetonitrile and insoluble in water and diethyl ether, except the silver(I) and mercury(II) complexes that are only soluble in DMSO and acetone.

4.3.1. [Cu(3)](BF₄)₂·5H₂O. Colour: brown. Yield 74%. Anal. Calcd for C₃₆H₃₆CuN₄O₁₆B₂F₈: C, 42.50; H, 3.56; N, 5.50. Found: C, 42.38; H, 3.80; N, 5.78; IR (cm⁻¹): 3458 ν(N–H)_{st}, 1637 ν(C=N)_{imin}, 1262 ν(C–O), 934 ν(C–O–C); MALDI-TOF-MS (*m/z*): 691.4 [(3)H]⁺; 754.3 [(3)Cu]⁺.

4.3.2. [Zn(3)](ClO₄)₂·1H₂O. Colour: orange. Yield 87%. Anal. Calcd for C₃₆H₂₈ZnN₄O₂₀Cl₂: C, 44.45; H, 2.90; N, 5.76. Found: C, 44.49; H, 2.80; N, 5.48; IR (cm⁻¹): 3457 ν(N–H)_{st}, 1645 ν(C=N)_{imin}, 1261 ν(C–O), 940 ν(C–O–C); MALDI-TOF-MS (*m/z*): 691.4 [(3)H]⁺; 755.2 [(3)Zn]⁺; 855.5 [(3)Zn(ClO₄)₂]⁺.

4.3.3. [Cd(3)](ClO₄)₂·6H₂O. Colour: yellow. Yield 84%. Anal. Calcd for C₃₆H₃₈CdN₄O₂₅Cl₂: C, 38.95; H, 3.45; N, 5.05. Found: C, 38.60; H, 3.80; N, 5.45; IR (cm⁻¹): 3445 ν(N–H)_{st}, 1649 ν(C=N)_{imin}, 1260 ν(C–O), 948 ν(C–O–C); MALDI-TOF-MS (*m/z*): 691.4 [(3)H]⁺; 803.2 [(3)Cd]⁺.

4.3.4. [Ag(3)](CF₃SO₃)₂·3H₂O. Colour: yellow. Yield 90%. Anal. Calcd for C₃₇H₃₂AgN₄O₁₇F₃S: C, 44.37; H, 3.22; N, 5.59. Found: C, 44.52; H, 3.34; N, 5.62; IR (cm⁻¹): 3442 ν(N–H)_{st}, 1643 ν(C=N)_{imin}, 1259 ν(C–O), 931 ν(C–O–C); MALDI-TOF-MS (*m/z*): 691.4 [(3)H]⁺; 799.8 [(3)Ag]⁺.

4.3.5. [Hg(3)](CF₃SO₃)₂·3H₂O. Colour: yellow-orange. Yield 72%. Anal. Calcd for C₃₈H₃₂AgN₄O₂₀F₆S₂: C, 36.71; H, 2.60; N, 4.50. Found: C, 36.52; H, 2.83; N, 4.62; IR (cm⁻¹): 3440 ν(N–H)_{st}, 1641 ν(C=N)_{imin}, 1260 ν(C–O), 931 ν(C–O–C); MALDI-TOF-MS (*m/z*): 691.4 [(3)H]⁺; 910.4 [(3)Hg]⁺.

4.4. Preparation of doped **(3)** PMMA polymer films

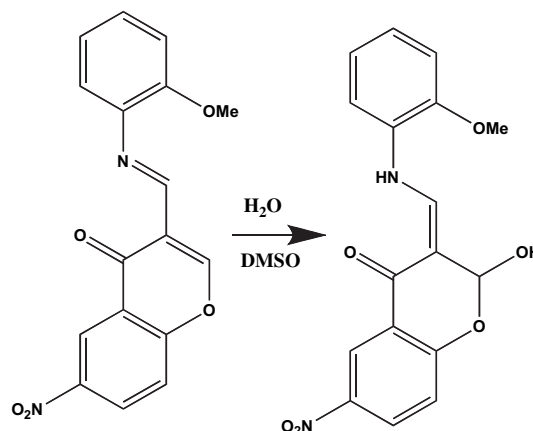
Polymethylmethacrylate (PMMA) is a common, low-cost, simply-prepared polymer with excellent optical quality. Preparation of the doped PMMA films was performed by a simple and easy method. The PMMA powder (0.1 g) was dissolved in chloroform PA, followed by addition of the compound **3** doped with 0.001–0.005 g dissolved in the same solvent. The polymer film was obtained after evaporation of solvent at 40 °C under vacuum for 24 h.²⁸

Due to the spectroscopic characteristics, the film doped with 0.005 g of **(3)** was selected for the studies with metal ions.

4.5. Computational methods

All calculations have been performed employing Density Functional Theory (DFT)²⁹ as implemented in the Gaussian 09 code.³⁰ Due to its remarkable performance for medium-size organic molecules, the M06-2X³¹ density functional was used along with the reasonably extended double-z quality 6-31+G(d,p) basis set. The stationary points obtained were confirmed to be minima by computation of the second derivatives of the energy with respect to the nuclei displacement. Solvation effects were taken into consideration through the polarizable dielectric continuum model (PCM) using DMSO parameters.³²

To reduce the computational cost of the hydration process a truncated system including a single cromene unit condensed with a 2-aminophenoxyethyl derivative has been employed (see Scheme 3).



Scheme 3. Truncated molecular system employed throughout the computational study.

Acknowledgements

Authors thank University of Vigo INOU-ViCou K914 and K915 (Spain) and Scientific PROTEOMASS Association (Ourense-Spain) for financial support. J.F.L. thanks Xunta de Galicia for his research contract in the aim of the Project 09CSA043383PR. C.N.; R.C.; H.M.S.; thank Fundação para a Ciência e a Tecnologia/FEDER (Portugal/EU) for the postdoctoral contract SFRH/BPD/65367/2009 and the doctoral grants SFRH/BP/28563/2006 and SFRH/BP/38509/2007, respectively. J.L.C., C.S.L. and C.L. thank Xunta de Galicia for the Isidro Parga Pondal Research programme.

Supplementary data

Supplementary data associated with this article can be found in the online version at doi:10.1016/j.tet.2010.11.040.

References and notes

- (a) Prodi, L.; Bolleta, F.; Montalti, M.; Zaccaroni, N. *Coord. Chem. Rev.* **2000**, *205*, 59; (b) Bren, V. A. *Chem. Rev.* **2001**, *70*, 1017; (c) Callan, J. F.; de Silva, A. P.; Magri, D. C. *Tetrahedron* **2005**, *61*, 8551.
- (a) Lodeiro, C.; Pina, F. *Coord. Chem. Rev.* **2009**, *253*, 1353; (b) de Silva, A. P.; Gunaratne, H. Q. N.; Gunnlaugsson, T.; Huxley, A. J. M.; McCoy, C. P.; Rademacher, J. T.; Rice, T. E. *Chem. Rev.* **1997**, *97*, 1515.
- Jain, N.; Kanojia, R. M.; Xu, J.; Jian-Zhong, G.; Pacia, E.; Lai, M.; Du, F.; Musto, A.; Allan, G.; Hahn, D.; Lundeen, S.; Sui, Z. *J. Med. Chem.* **2006**, *49*, 3056.
- Nicolaou, K. C.; Pfefferkorn, J. A.; Roecker, A. J.; Cao, G.-Q.; Barluenga, S.; Mitchell, H. J. *J. Am. Chem. Soc.* **2000**, *122*, 9939.
- Nicolaou, K. C.; Pfefferkorn, J. A.; Mitchell, H. J.; Roecker, A. J.; Barluenga, S.; Cao, G.-Q.; Affleck, R. L.; Lillig, J. E. *J. Am. Chem. Soc.* **2000**, *122*, 9954.
- Nicolaou, K. C.; Pfefferkorn, J. A.; Barluenga, S.; Mitchell, H. J.; Roecker, A. J.; Cao, G.-Q. *J. Am. Chem. Soc.* **2000**, *122*, 9968.
- Zeni, G.; Larock, R. C. *Chem. Rev.* **2004**, *104*, 2285.
- Mori, J.; Iwashima, M.; Takeuchi, M.; Saito, H. *Chem. Pharm. Bull.* **2006**, *54*, 391.
- Kashiwada, Y.; Yamazaki, K.; Ikeshiro, Y.; Yamasibi, T.; Fujioka, T.; Milashi, K.; Mizuki, K.; Cosentino, L. M.; Fowke, K. S.; Natschke, L. M.; Lee, K.-H. *Tetrahedron* **2001**, *57*, 1559.
- Foye, W. O. *Principi Di Chemico Farmaceutica*; Piccin: Padova, Italy, 1991; p 416.
- Bonsignore, L.; Loy, G.; Secci, D.; Calignano, A. *Eur. J. Med. Chem.* **1993**, *28*, 517.
- Gáplóvský, A.; Donovalová, J.; Lácová, M.; Mračnová, R.; El-Shaar, H. M. *J. Photochem. Photobiol., A* **2000**, *136*, 61.
- Huo, F.; Sun, Y.; Su, J.; Chao, J.; Zhi, H.; Yin, C. *Org. Lett.* **2009**, *11*, 4918.
- Gosh, C. K. *J. Heterocycl. Chem.* **1983**, *20*, 1437.
- (a) Sabitha, G. *Aldrichimica Acta* **1996**, *29*, 15.
- Lodeiro, C.; Capelo, J. L.; Mejuto, J. C.; Oliveira, E.; Santos, H. M.; Pedras, B.; Nuñez, C. *Chem. Soc. Rev.* **2010**, *39*, 2948.
- (a) Tasker, P. A.; Fleisher, Y. E. B. *J. Am. Chem. Soc.* **1970**, *92*, 7072; (b) Vicente, M.; Lodeiro, C.; Adams, H.; Bastida, R.; de Blás, A.; Fenton, D. E.; Macías, A.; Rodríguez, A.; Rodríguez-Blás, T. *Eur. J. Inorg. Chem.* **2000**, *6*, 1015.
- El, B.; Slawomir, P. *Tetrahedron* **1999**, *55*, 4815.
- Raj, T.; Bhatia, R. K.; Kapur, A.; Sharma, M.; Saxena, A. K.; Ishar, M. P. S. *Eur. J. Med. Chem.* **2010**, *45*, 790.
- Ortica, F.; Bougdid, L.; Moustrou, C.; Mazzucato, U.; Favaro, G. *J. Photochem. Photobiol. A. Chem.* **2008**, *200*, 287.
- Lakowicz, R. J. *Topics in Fluorescence Spectroscopy. Probe Design and Chemical Sensing*; Kluwer Academica: New York, NY, 2002; Vol. 4.
- Rurack, K. *Spectrochim. Acta, Part A* **2001**, *57*, 2161.
- Fernandes, L.; Boucher, M.; Fernández-Lodeiro, J.; Oliveira, E.; Nuñez, C.; Santos, H. M.; Capelo, J. L.; Nieto-Faza, O.; Bértolo, E.; Lodeiro, C. *Inorg. Chem. Commun.* **2009**, *12*, 905.
- Gans, P.; Sabatini, A.; Vacca, A. *Talanta* **1996**, *43*, 1739.
- (a) McGehee, M. D.; Bergstedt, T.; Zhang, C.; Saab, A. P.; O'Regan, M. B.; Bazan, G. C.; Srdanov, V. I.; Heeger, A. J. *Adv. Mater.* **1999**, *11*, 1349; (b) Balamurugan, A.; Reddy, M. L. P.; Jayakannan, M. *J. Phys. Chem. B* **2009**, *113*, 14128; (c) Boyer, J. C.; Johnson, N. J. J.; van Veggel, F. C. J. M. *Chem. Mater.* **2009**, *21*, 2010; (d) Kai, J.; Parrab, D. F.; Brito, H. F. *J. Mater. Chem.* **2008**, *18*, 4549; (e) Zhang, H.; Song, H.; Dong, B.; Han, L.; Pan, G.; Bai, X.; Fan, L.; Lu, S.; Zhao, H.; Wang, F. *J. Phys. Chem. C* **2008**, *112*, 9155.
- Hillenkamp, F.; Peter-Katalinić, J. *A Practical Guide to Instrumentation Methods and Applications*; Wiley: Germany, 2007, pp 18–20.
- Berlman, I. B. *Handbook of Fluorescence Spectra of Aromatic Molecules*, 2nd ed.; Academic: New York, NY, 1971.
- (a) Raj, D. B. A.; Francis, B.; Reddy, M. L. P.; Butorac, R. R.; Lynch, V. M.; Cowley, A. H. *Inorg. Chem.* **2010**, *49*, 9055; (b) Moudam, O.; Rowan, B. C.; Alamiry, M.; Richardson, P.; Richards, B. S.; Jones, A. C.; Robertson, N. *Chem. Commun.* **2009**, 6649.
- (a) Hohenberg, P.; Kohn, W. *Phys. Rev.* **1964**, *136*, B864; (b) Kohn, W.; Sham, L. *Phys. Rev.* **1965**, *140*, A1133.
- Frisch, M. J.; Trucks, G. W.; Schlegel, H. B.; Scuseria, G. E.; Robb, M. A.; Cheeseman, J. R.; Scalmani, G.; Barone, V.; Mennucci, B.; Petersson, G. A.; Nakatsuji, H.; Caricato, M.; Li, X.; Hratchian, H. P.; Izmaylov, A. F.; Bloino, J.; Zheng, G.; Sonnenberg, J. L.; Hada, M.; Ehara, M.; Toyota, K.; Fukuda, R.; Hasegawa, J.; Ishida, M.; Nakajima, T.; Honda, Y.; Kitao, O.; Nakai, H.; Vreven, T.; Montgomery, J. A., Jr.; Peralta, J. E.; Ogliaro, F.; Bearpark, M.; Heyd, J. J.; Brothers, E.; Kudin, K. N.; Staroverov, V. N.; Kobayashi, R.; Normand, J.; Raghavachari, K.; Rendell, A.; Burant, J. C.; Iyengar, S. S.; Tomasi, J.; Cossi, M.; Rega, N.; Millam, N. J.; Klene, M.; Knox, J. E.; Cross, J. B.; Bakken, V.; Adamo, C.; Jaramillo, J.; Gomperts, R.; Stratmann, R. E.; Yazyev, O.; Austin, A. J.; Cammi, R.; Pomelli, C.; Ochterski, J. W.; Martin, R. L.; Morokuma, K.; Zakrzewski, V. G.; Voth, G. A.; Salvador, P.; Dannenberg, J. J.; Dapprich, S.; Daniels, A. D.; Farkas, Ö.; Foresman, J. B.; Ortiz, J. V.; Cioslowski, J.; Fox, D. J. *Gaussian 09, Revision A.1*; Gaussian: Wallingford CT, 2009.
- Zhao, Y.; Truhlar, D. G. *Theor. Chem. Acc.* **2007**, *120*, 215.
- (a) Tomasi, J.; Persico, M. *Chem. Rev.* **1994**, *94*, 2027; (b) Mineva, T.; Russo, N.; Sicilia, E. *J. Comput. Chem.* **1998**, *19*, 290; (c) Cossi, M.; Scalmani, G.; Rega, N.; Barone, V. *J. Chem. Phys.* **2002**, *117*, 43.